blood advances

Hemojuvelin-mediated hepcidin induction requires both bone morphogenetic protein type I receptors ALK2 and ALK3

Deniz Y. Dogan,[1,2] Eugen I. Urzica,[3] Isabelle Hornung,[1] Philipp Kastl,[4] David Oguama,[3] Franca M. Fette,[3] Lien H. Nguyen,[3] Frank Rosenbauer,[5] Kai Zacharowski,[1] Ursula Klingmüller,[4] Elise Gradhand,[6] Andreas von Knethen,[1] Rüdiger Popp,[7] Ingrid Fleming,[7,8] Lisa Schrader,[1,3,*] and Andrea U. Steinbicker[1,3,*]

[1]Department of Anesthesiology, Goethe University Frankfurt, Intensive Care Medicine and Pain Therapy, University Hospital Frankfurt, Frankfurt, Germany; [2]Department of Psychiatry and Psychotherapy, Campus Benjamin Franklin, Charité-Universitätsmedizin Berlin, Humboldt-Universität zu Berlin, and Berlin Institute of Health, Berlin, Germany; [3]Department of Anesthesiology, Intensive Care and Pain Medicine, University Hospital Muenster, University of Muenster, Muenster, Germany; [4]Division Systems Biology of Signal Transduction, German Cancer Research Center, Heidelberg, Germany; [5]Institute of Molecular Tumor Biology, University Hospital Muenster, University of Muenster, Muenster, Germany; [6]Senckenberg Institute for Pathology, University Hospital Frankfurt and [7]Institute for Vascular Signalling, Centre for Molecular Medicine, Goethe University, Frankfurt, Germany; and [8]German Centre for Cardiovascular Research Partner Site Rhein Main, Frankfurt, Germany

Key Points

- The bone morphogenetic protein type I receptors ALK2 and ALK3 are required for HJV-mediated induction of hepcidin in vivo.

Hemojuvelin (HJV) is a glycosylphosphatidylinositol-anchored protein of the repulsive guidance molecule family acting as a bone morphogenetic protein (BMP) coreceptor to induce the hepatic iron regulatory protein hepcidin. Hepcidin causes ubiquitination and degradation of the sole known iron exporter ferroportin, thereby limiting iron availability. The detailed signaling mechanism of HJV in vivo has yet to be investigated. In the current manuscript, we used an established model of adeno-associated virus (AAV)-mediated liver-specific overexpression of HJV in murine models of hepatocyte-specific deficiency of the BMP type I receptors *Alk2* or *Alk3*. In control mice, HJV overexpression increased hepatic *Hamp* messenger RNA (mRNA) levels, soluble HJV (sHJV), splenic iron content (SIC), as well as phosphorylated small mothers against decapentaplegic protein (pSMAD1/5/8) levels. In contrast, in *Alk2fl/fl;Alb-Cre* and *Alk3fl/fl;Alb-Cre* mice, which present with moderate and severe iron overload, respectively, the administration of AAV-HJV induced HJV and sHJV. However, it did not rescue the iron overload phenotypes of those mice. Serum iron levels were induced in *Alk2fl/fl;Alb-Cre* mice after HJV overexpression. In phosphate-buffered saline–injected *Alk3fl/fl;Alb-Cre* mice, serum iron levels and the expression of duodenal ferroportin remained high, whereas *Hamp* mRNA levels were decreased to 1% to 5% of the levels detected in controls. This was reduced even further by AAV-HJV overexpression. SIC remained low in mice with hepatocyte-specific *Alk2* or *Alk3* deficiency, reflecting disturbed iron homeostasis with high serum iron levels and transferrin saturation and an inability to induce hepcidin by HJV overexpression. The data indicate that ALK2 and ALK3 are both required in vivo for the HJV-mediated induction of hepcidin.

The full-text version of this article contains a data supplement.

Introduction

Iron homeostasis requires a multitude of regulatory mechanisms including different iron regulatory proteins. The hepatic hormone hepcidin is the key regulatory protein that controls systemic iron homeostasis.[1] The main erythroid regulator of hepcidin is erythroferrone (ERFE).[2] ERFE controls plasma iron levels and total body iron. It is induced by erythropoietin in the kidney and inhibits hepcidin by binding to bone morphogenetic protein (BMP) ligands, thereby limiting BMP receptor activation.[3] Hepcidin induces the ubiquitination and degradation of the sole known iron exporter ferroportin, thereby reducing iron uptake from the diet and iron release from hepatocytes and macrophages.[4] Hepcidin is produced in the liver in response to circulating and stored iron and inflammatory mediators such as interleukin-6. At the transcriptional level, the expression of hepcidin is controlled by the BMP-SMAD (small mothers against decapentaplegic protein) signaling pathway.[5] In hepatocytes, this pathway is activated by BMP2 and BMP6 ligands that are secreted by liver sinusoidal endothelial cells.[6] Upon binding of BMP2 and/or BMP6 to the BMP receptor complex, BMP type II receptors phosphorylate the BMP type I receptors ALK2 and ALK3, which are known to form ALK2/ALK3 heterodimers, ALK3/ALK3 homodimers, and ALK2/ALK2 homodimers.[7-9] Both, ALK2 and ALK3 are required for BMP2-, BMP6-, and BMP2/6-mediated hepcidin induction.[3,8,10] Hemojuvelin (HJV) is a glycosylphosphatidylinositol (GPI)-anchored protein of the repulsive guidance molecule family that acts as a BMP coreceptor.[11] Mutations in the gene encoding *Hjv* lead to markedly reduced hepcidin levels and thus cause severe iron overload in humans.[12] HJV directly binds BMP ligands and activates BMP signaling.[11,13] HJV exists in 2 forms: GPI membrane–anchored HJV and soluble plasmatic HJV (sHJV). Already, in 2007, Babitt et al showed that BMP ligands induce hepcidin but that sHJV at increasing concentrations leads to a decrease in hepcidin expression by binding of sHJV to BMP ligands.[14]

A model by Healey et al, based on in vitro and in silico experiments, suggests that HJV forms a complex with BMP ligands, which is targeted to endosomes. In endosomes, HJV dissociates from BMP ligands and is replaced by BMP type I receptors for downstream signaling.[15] The exact mechanism by which HJV enhances BMP signaling is still under investigation. It has been shown that BMP2 has competing binding sites at HJV and the ectodomain of ALK3.[15]

To further elucidate, which BMP type I receptor(s) are used by HJV to activate BMP signaling in vivo and to elucidate the effects of HJV overexpression on systemic iron homeostasis, we studied the consequences of adeno-associated virus (AAV)-mediated overexpression of HJV as well as the impact of the hepatocyte-specific deficiency of *Alk2* or *Alk3*.[8] The data indicate that HJV mediated induction of hepcidin requires both receptors, ALK2 and ALK3, in vivo.

Material and methods

Animals

Animal protocols were approved by the institutional ethical committee of the North Rhine-Westphalian Agency for Nature, Environment, and Consumer Protection (permit number Az. 81.92.04.2019.A207). Hepatocyte-specific *Alk2-* (*Alk2fl/fl;Alb-Cre*) or *Alk3*-deficient (*Alk3fl/fl;Alb-Cre*) mice and *Cre-* control littermates on a C57BL/6 background[16,17] were fed a standard rodent diet (198 parts per million iron). Eight-week-old male mice were injected intravenously with either 5×10^{11} particles of AAV2/8 expressing *Hjv-MycDDK* under the control of a liver-specific promoter (AAV2/8-ALB-*mHfe2-MycDDK*, abbreviated as AAV-HJV; supplemental Figure 1) (Vector BioLabs) or phosphate-buffered saline (PBS) as control.[18] PBS was used as control because it has been shown that an AAV2/8 expressing glutaryl-coenzyme A dehydrogenase (a protein unrelated to iron homeostasis) did not cause an induction of inflammatory parameters nor did it affect iron homeostasis.[19] Mice were euthanized 2 weeks after virus administration under deep anesthesia, and blood and organs were collected for further analysis.

Hepcidin, hematologic, and iron parameters

Blood was drawn by retro-orbital puncture under deep ketamine/xylazine anesthesia. Serum iron levels and unsaturated binding capacity were determined using the Iron/U.I.B.C Kit (Biolabo) according to the manufacturer's instructions. Hepcidin levels were determined using the Hepcidin Murine-Compete enzyme-linked immunosorbent assay kit (Intrinsic Lifesciences) according to the manufacturer's instructions. Nonheme tissue iron content was determined as described by Torrance and Bothwell.[20] For histological staining of nonheme iron, paraffin embedded tissue sections (4 μm) were stained with Perls' Prussian blue stain.

qRT-PCR

Total RNA was extracted from tissue samples using Trizol (Sigma-Aldrich) according to the manufacturer's instructions. Complementary DNA was synthesized using MMLV-reverse transcriptase (Sigma-Aldrich). Quantitative real-time polymerase chain reaction (qRT-PCR) was performed on the Bio-Rad CFX Connect real-time PCR system using either iTaq Universal SYBR Green supermix (BioRad) or TaqMan universal master mix (Applied Biosystems). TaqMan probes and primer pairs are listed in supplemental Table 1. Target gene expression was normalized to levels of 18S ribosomal RNA and calculated using the relative C_T method.[21]

Immunoblotting and iron staining

Tissue samples were lysed in RIPA buffer supplemented with protease and phosphatase inhibitor cocktails, and protein concentration was determined using the Pierce bicinchoninic acid protein assay kit (Thermo Fisher Scientific). Equal amounts of isolated proteins from tissue samples were separated by electrophoresis using 10% to 16% bis- tris(hydroxymethyl)aminomethane gels. Proteins were transferred on nitrocellulose membranes and incubated with antibodies directed against glyceraldehyde-3-phosphate dehydrogenase (no. G8795, Sigma-Aldrich), HJV (no. AF3634, R&D Systems), ferroportin (no. NBP1-21502, Novus Biologicals), or pSMAD1,5,9 (no. Vl131, Maine Medical Center Research Institute), and Li-Cor secondary antibodies (no. 926-32210 800CW goat anti-mouse immunoglobulin G, no. 926-68073 680RD donkey anti-rabbit immunoglobulin G). Immunoblots were imaged using the LI-COR Odyssey DLx imaging system (LI-COR).

For iron staining of formalin-fixed, paraffin-embedded material, 4-μm-thick slides were stained with 10% potassium hexacyanoferate (Roth). Hematoxylin and eosin–stained slides and FE-stained slides

(Perls' stain) were examined with an optical/light microscope (Scope A1, Zeiss)

Immunofluorescence

Duodenal sections were deparaffinized and blocked (1 hour at room temperature) with PBS containing 5% horse serum and 0.3% Triton X-100, and then incubated overnight (4°C) with a primary antibody directed against ferroportin (no. NBP1-21502, Novus Biologicals). Thereafter, slides were washed with PBS and incubated (2 hours at room temperature) with the corresponding secondary antibody Alexa Fluor 546 (no. A10040, Thermo Fisher Scientific). After repetitive washing with PBS, slides were mounted in glycerin-based Hoechst 33347 containing mounting medium (Sigma-Aldrich). Images were generated using a Zeiss confocal microscope (LSM 780, Zeiss) and were analyzed with Imaris 10.1 (Bitplane) using the surface rendering function to quantify the area of fluorescence signal normalized to area of field view.

Statistical analysis

All data are presented as box plots with individual data points shown and medians. Equality of variances was validated by Levene test and outliers by Grubbs test. The Shapiro-Wilk test was performed to test for normality. Means were compared by Students t test and 1-way analysis of variance or Welch analysis of variance for parametric data, and Mann-Whitney U test and Kruskal Wallis test for nonparametric data sets (Prism 8, GraphPad Software). A P value <.05 was considered statistically significant. Correlations were analyzed using nonparametric Spearman correlation with a 2-tailed P value.

Results

Successful liver-specific overexpression of HJV by AAV-HJV in vivo

Because deficiency of HJV reduces BMP signaling and hepcidin expression and leads to the development of severe iron overload in mice,[12] we sought to investigate the role of BMP signaling in HJV induction. Previous studies have shown that the BMP type I receptors ALK2 and ALK3 are crucial for the expression of hepcidin and iron homeostasis.[8]

To investigate whether activation of BMP/SMAD signaling and induction of hepcidin expression by HJV are dependent on the BMP type I receptor ALK2 and/or ALK3, mice with hepatocyte-specific deficiency for *Alk2* or *Alk3* were injected with an AAV2/8 expressing *HJV-Myc-DDK* under the control of a liver-specific promoter or PBS as a control. Fourteen days after virus administration, blood and organs were harvested and the effect of HJV overexpression on iron parameters and hepcidin expression was investigated. First, the efficiency of *Alk2* or *Alk3* knockdown and of HJV overexpression were verified. Hepatocyte-specific *Alk2*-deficient mice had an 84% reduction in *Alk2* messenger RNA (mRNA) levels compared with control mice, and hepatocyte-specific *Alk3*-deficient mice had a 93% reduction in *Alk3* mRNA levels compared with control mice (Figure 1A-B). The successful in vivo, liver-specific AAV-HJV–mediated overexpression of HJV was confirmed by qRT-PCR and immunoblotting (Figure 1C-D; also previously reported[22]). It has been previously published that HJV-Myc-DDK is detected in membrane-enriched fractions of the liver of animals injected with AAV-HJV[22] (Figure 1D). In control mice

and in mice with hepatocyte-specific *Alk2* or *Alk3* deficiency, hepatic *Hjv* mRNA and HJV protein levels (in the form of 2 bands, as described previously[22]) were increased to a similar extent (Figure 1C; supplemental Figure 2). HJV was not detected in a hepatic sample of a *Hjv*-knockout mouse (supplemental Figure 2C). Liver-specific targeting of AAV2/8[23] was confirmed by lack of HJV protein expression in the spleen (supplemental Figure 2D). The data indicate that all mice injected with AAV-HJV were successfully overexpressing HJV in the liver in vivo.

HJV overexpression induced hepcidin levels in control mice

To investigate the effect of HJV overexpression on BMP signaling, hepatic *Hamp* mRNA and serum hepcidin levels were determined. The overexpression of HJV increased hepatic *Hamp* mRNA levels in control mice injected with AAV-HJV compared with PBS-injected control mice (Figure 2A). In *Alk2^{fl/fl};Alb-Cre* mice the basal expression of *Hamp* mRNA was not altered, but HJV overexpression resulted in slightly reduced *Hamp* mRNA expression, albeit not significant. However, in *Alk3^{fl/fl};Alb-Cre* mice baseline *Hamp* mRNA expression was already heavily reduced, which was further suppressed by the administration of AAV-HJV (inlay, Figure 2A).

There is a positive correlation between hepatic *Hamp* mRNA levels and *Hjv* mRNA levels in control mice (R = 0.66; supplemental Figure 3A), whereas hepatic *Hamp* mRNA levels and *Hjv* mRNA levels negatively correlated in *Alk2^{fl/fl};Alb-Cre* and *Alk3^{fl/fl};Alb-Cre* mice (R = −0.44; supplemental Figure 3B). The data indicated a dependency of HJV and hepcidin that is absent in mice with a deficiency of either of the 2 BMP type I receptors *Alk2* or *Alk3*. Serum hepcidin levels were also measured and showed a similar trend as that of the *Hamp* mRNA levels, albeit differences were not statistically significant (Figure 2B).

In order to show that HJV overexpression induces hepcidin levels by activation of the BMP signaling pathway, the phosphorylation of SMAD1/5/8 proteins and the expression levels of the BMP target gene *Id1* were investigated. pSMAD1/5/8 protein levels were mildly increased in AAV-HJV control mice when compared with PBS-injected mice, whereas there was little signaling activity in *Alk2^{fl/fl};Alb-Cre* mice and no activity in *Alk3^{fl/fl};Alb-Cre* mice (Figure 2C; supplemental Figure 3C), which confirmed our previous finding that *Alk3^{fl/fl};Alb-Cre* mice are characterized by very low pSMAD1/5/8 levels.[8] The expression levels of *Id1* were increased in control mice injected with AAV-HJV, whereas the administration of AAV-HJV had no effect on *Id1* mRNA levels in *Alk2^{fl/fl};Alb-Cre* and *Alk3^{fl/fl};Alb-Cre* mice (Figure 2D). Because hepcidin directly regulates the surface expression of ferroportin, we assessed its level in intestine using immunofluorescence and confocal microscopy (Figure 2E-F). In untreated control mice ferroportin was barely detectable (Figure 2E, top panel); despite this, ferroportin level tended to decrease after the application of AAV-HJV (Figure 2F). In mice lacking ALK3 in hepatocytes (*Alk3^{fl/fl};Alb-Cre* mice) ferroportin levels were markedly increased because of hepcidin deficiency (Figure 2E, bottom). *Hamp* mRNA was even further decreased in the latter mice after HJV injection, and ferroportin protein levels remained high (Figure 2F). The data indicate that HJV overexpression induces hepcidin in control mice but not in *Alk2^{fl/fl};Alb-Cre* and *Alk3^{fl/fl};Alb-Cre* mice by activation of the BMP-SMAD
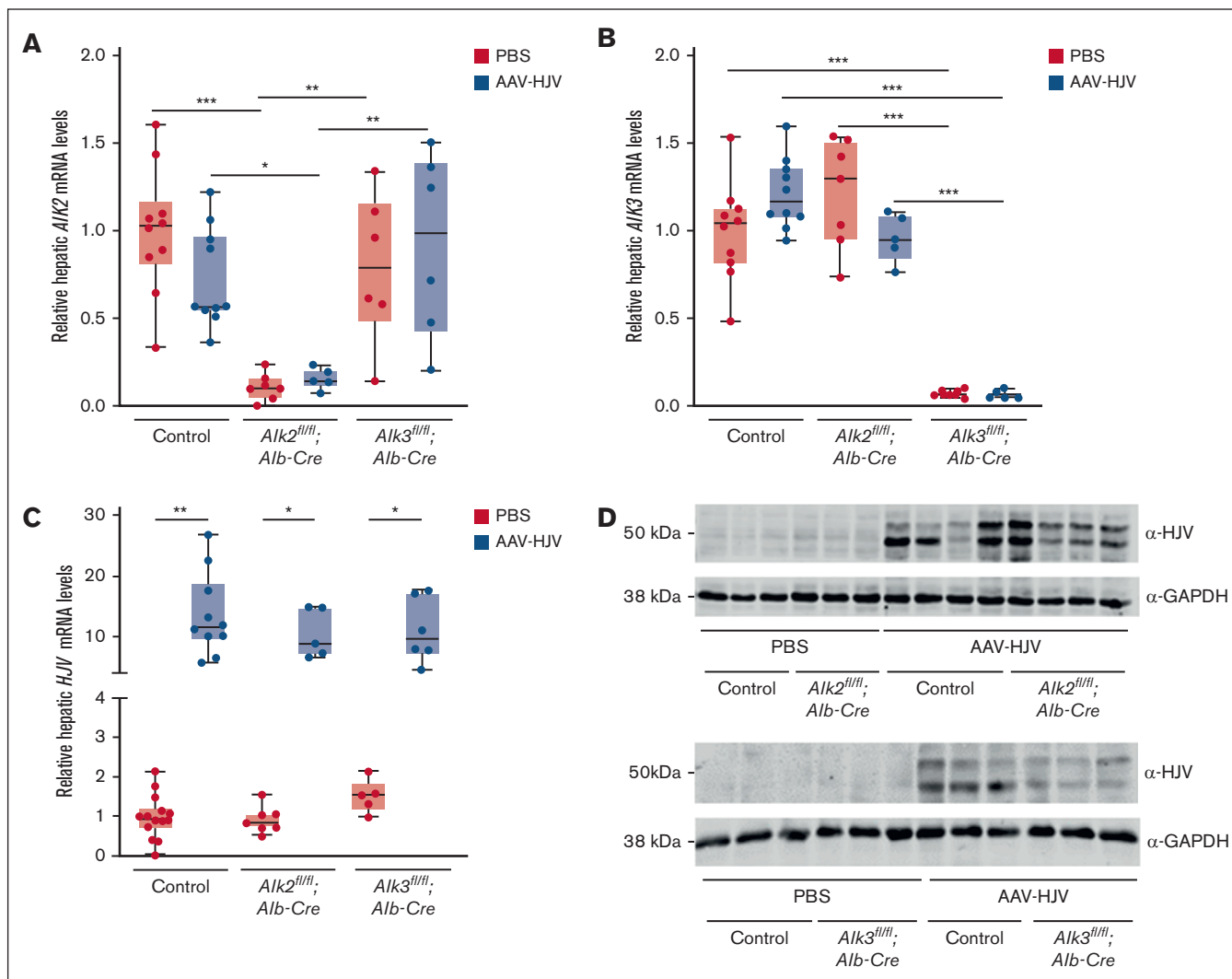
Figure 1. Intravenous AAV2/8-ALB-*mHFE2-MycDDK* (abbreviated as *AAV-HJV*) injection induces liver-specific HJV expression. Hepatocyte-specific *Alk2*-deficient mice (*Alk2^{fl/fl};Alb-Cre*), hepatocyte-specific *Alk3*-deficient mice (*Alk3^{fl/fl};Alb-Cre*), and their respective controls (*Alk2^{fl/fl}* or *Alk3^{fl/fl}*; ≥5 mice per group) at 8 weeks of age were intravenously injected with 5×10^{11} particles of an AAV2/8 expressing *Hjv-MycDDK* under the control of a liver-specific promotor or PBS, and euthanized 2 weeks later. (A) *Alk2* mRNA levels (control PBS, n = 10; control AAV-HJV, n = 10; *Alk2^{fl/fl};Alb-Cre* PBS, n = 7; *Alk2^{fl/fl};Alb-Cre* AAV-HJV, n = 5; *Alk3^{fl/fl};Alb-Cre* PBS, n = 6; and *Alk3^{fl/fl};Alb-Cre* AAV-HJV, n = 6) and (B) *Alk3* mRNA levels in the liver were determined by qRT-PCR to verify knockdown efficiency. 18S ribosomal RNA was used as an internal control (control PBS, n = 10; control AAV-HJV, n = 10; *Alk2^{fl/fl};Alb-Cre* PBS, n = 7; *Alk2^{fl/fl};Alb-Cre* AAV-HJV, n = 5; *Alk3^{fl/fl};Alb-Cre* PBS, n = 6; and *Alk3^{fl/fl};Alb-Cre* AAV-HJV, n = 6). (C) Relative hepatic *Hjv* mRNA levels were determined by qRT-PCR. Transcripts were normalized to 18S ribosomal RNA, and the average of control mice treated with PBS was set to 1 (control PBS, n = 14; control AAV-HJV, n = 10; *Alk2^{fl/fl};Alb-Cre* PBS, n = 7; *Alk2^{fl/fl};Alb-Cre* AAV-HJV, n = 5; *Alk3^{fl/fl};Alb-Cre* PBS, n = 5; and *Alk3^{fl/fl};Alb-Cre* AAV-HJV, n = 6). (D) HJV protein levels were determined to validate the hepatic overexpression of HJV. Glyceraldehyde-3-phosphate dehydrogenase (GAPDH) was used as internal control. Data are presented as box plots with minimum to maximum whiskers. Significances were presented relative to the indicated control with *$P < .05$, **$P < .01$, and ***$P < .001$. (*Alk2^{fl/fl}* PBS, n = 3; *Alk2^{fl/fl};Alb-Cre* PBS, n = 3; *Alk2^{fl/fl}* AAV-HJV, n = 4; *Alk2^{fl/fl};Alb-Cre* AAV-HJV, n = 4; *Alk3^{fl/fl}* PBS, n = 3; *Alk3^{fl/fl};Alb-Cre* PBS, n = 3; *Alk3^{fl/fl}* AAV-HJV, n = 3; and *Alk3^{fl/fl};Alb-Cre* AAV-HJV, n = 3).

signaling pathway. Interestingly, the loss of BMP signal transduction in *Alk2^{fl/fl};Alb-Cre* and *Alk3^{fl/fl};Alb-Cre* mice could not be rescued by HJV overexpression, but rather this abolished the positive correlation of HJV to hepcidin that was detected in control mice injected with AAV-HJV.

Effect of HJV overexpression on iron homeostasis

Hepcidin is the major regulator of systemic iron homeostasis and overexpression of HJV induced hepcidin levels in controls but not in *Alk2^{fl/fl};Alb-Cre* and *Alk3^{fl/fl};Alb-Cre* mice. Because hepatocyte-specific *Alk2* and *Alk3* deficiency causes moderate and severe iron overload, respectively,[8] we investigated the effect of HJV overexpression on systemic iron homeostasis, serum iron parameters, and tissue iron contents in *Alk2^{fl/fl};Alb-Cre* and *Alk3^{fl/fl};Alb-Cre* mice.

Serum iron levels and transferrin saturation were unchanged, with a slight trend to a reduction in control animals upon overexpression of HJV- compared with PBS-injected animals (Figure 3A-B). In *Alk2^{fl/fl};Alb-Cre* mice, the injection of AAV-HJV resulted in the
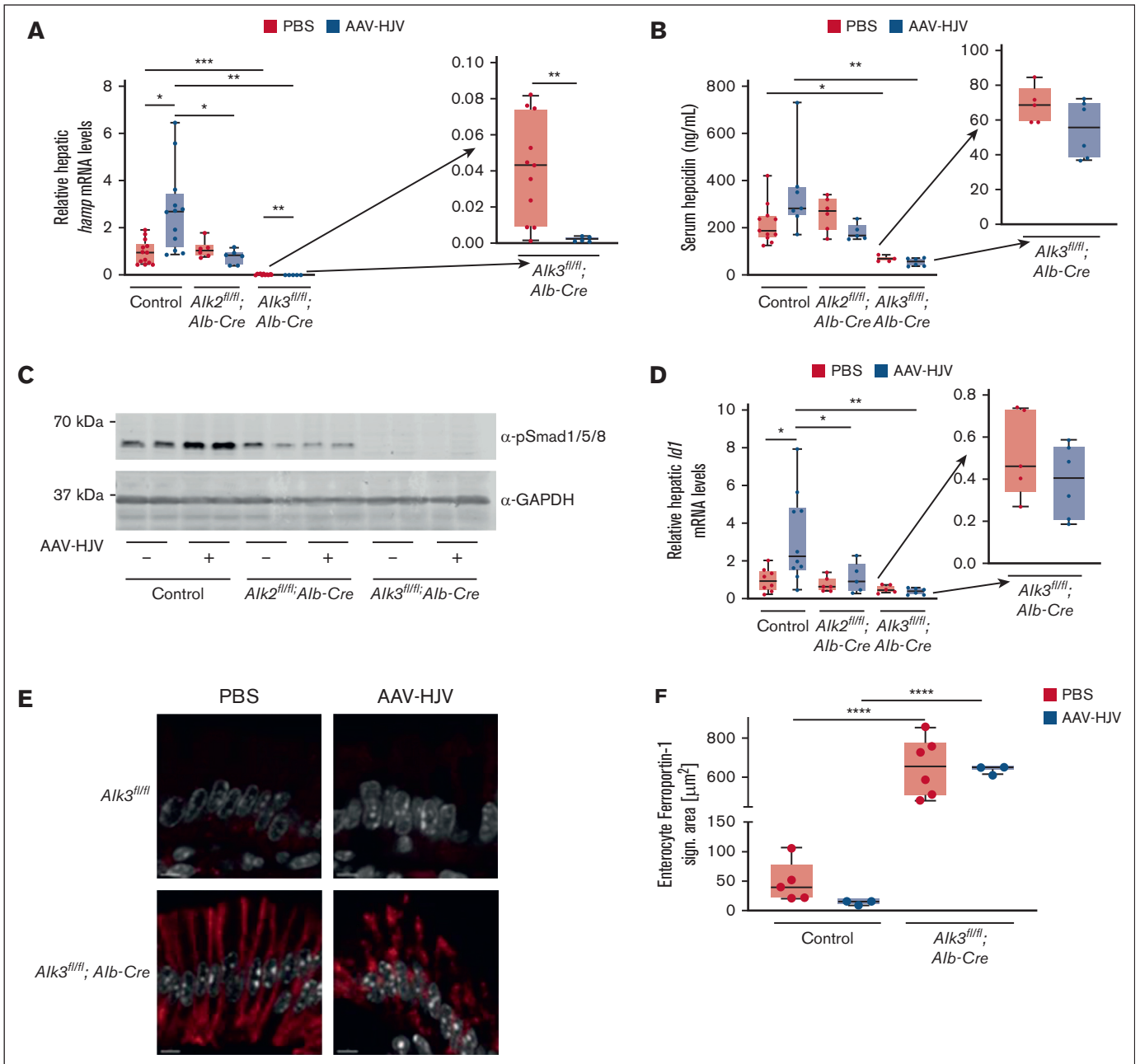
Figure 2. HJV overexpression in control animals induced BMP signaling and increased hepcidin expression. (A) Relative hepatic hepcidin (*Hamp*) mRNA levels were determined by qRT-PCR. Transcripts were normalized to 18S ribosomal RNA as internal controls, and the average of respective *Alk2^fl/fl^* and *Alk3^fl/fl^* control mice was set to 1 (control PBS, n = 13; control AAV-HJV, n = 12; *Alk2^fl/fl^;Alb-Cre* PBS, n = 6; *Alk2^fl/fl^;Alb-Cre* AAV-HJV, n = 6; *Alk3^fl/fl^;Alb-Cre* PBS, n = 11; and *Alk3^fl/fl^;Alb-Cre* AAV-HJV, n = 5). (B) Serum hepcidin levels were decreased in hepatocyte-specific *Alk3*-deficient mice compared with control animals as determined by enzyme-linked immunosorbent assay (control PBS, n = 11; control AAV-HJV, n = 7; *Alk2^fl/fl^;Alb-Cre* PBS, n = 6; *Alk2^fl/fl^;Alb-Cre* AAV-HJV, n = 5; *Alk3^fl/fl^;Alb-Cre* PBS, n = 5; and *Alk3^fl/fl^;Alb-Cre* AAV-HJV, n = 6). (C) HJV overexpression in control animals increased the level of pSMAD1/5/8 determined by immunoblotting. GAPDH was used as a loading control. (D) Hepatic *Id1* mRNA levels were determined by qRT-PCR. Transcripts were normalized to 18S ribosomal RNA, and the average of control mice treated with PBS was set to 1 (control PBS, n = 8; control AAV-HJV, n =10; *Alk2^fl/fl^;Alb-Cre* PBS, n = 6; *Alk2^fl/fl^;Alb-Cre* AAV-HJV, n = 5; *Alk3^fl/fl^;Alb-Cre* PBS, n = 5; and *Alk3^fl/fl^;Alb-Cre* AAV-HJV, n = 6). (E) Ferroportin staining (red) and DAPI (4′,6-diamidino-2-phenylindole) staining (white) of representative duodenal sections of control mice and *Alk3^fl/fl^;Alb-Cre* mice injected with PBS or AAV-HJV are shown. (F) In *Alk3^fl/fl^;Alb-Cre* mice the ferroportin signal is increased compared with control littermates. AAV-HJV injection in control mice decreased the ferroportin signal, albeit not significant. In *Alk3^fl/fl^;Alb-Cre* mice there is no difference in ferroportin signal detectable between AAV-HJV–injected mice and PBS-injected mice (control PBS, n = 5; control AAV-HJV, n = 3; *Alk3^fl/fl^;Alb-Cre* PBS, n = 6; and *Alk2^fl/fl^;Alb-Cre* AAV-HJV, n = 3). Data are presented as box plots with minimum to maximum whiskers and medians. Significances were presented relative to the indicated control with *$P < .05$, **$P < .01$, ***$P < .001$, and ****$P < .0001$.

Figure 3. HJV overexpression affects iron homeostasis in mice. (A) Serum iron levels (control PBS, n = 8; control AAV-HJV, n = 5; *Alk2*^{fl/fl};*Alb-Cre* PBS, n = 6; *Alk2*^{fl/fl};*Alb-Cre* AAV-HJV, n = 5; and *Alk3*^{fl/fl};*Alb-Cre* PBS, n = 5; and *Alk3*^{fl/fl};*Alb-Cre* AAV-HJV, n = 6) and (B) transferrin saturation were determined to analyze systemic iron homeostasis (control PBS, n = 9; control AAV-HJV, n = 5; *Alk2*^{fl/fl};*Alb-Cre* PBS, n = 6; *Alk2*^{fl/fl};*Alb-Cre* AAV-HJV, n = 5; *Alk3*^{fl/fl};*Alb-Cre* PBS, n = 5; and *Alk3*^{fl/fl};*Alb-Cre* AAV-HJV, n = 6). (C) Liver iron content was measured to determine tissue iron retention (control PBS, n = 11; control AAV-HJV, n = 9; *Alk2*^{fl/fl};*Alb-Cre* PBS, n = 7; *Alk2*^{fl/fl};*Alb-Cre* AAV-HJV, n = 5; *Alk3*^{fl/fl};*Alb-Cre* PBS, n = 6; and *Alk3*^{fl/fl};*Alb-Cre* AAV-HJV, n = 6). (D) Hepatic *Bmp6* mRNA levels were determined by qRT-PCR. 18S ribosomal RNA was used as an internal control and the average of control mice treated with PBS was set to 1 (control PBS, n = 10; control AAV-HJV, n = 10; *Alk2*^{fl/fl};*Alb-Cre* PBS, n = 7; *Alk2*^{fl/fl};*Alb-Cre* AAV-HJV, n = 5; *Alk3*^{fl/fl};*Alb-Cre* PBS, n = 6; and *Alk3*^{fl/fl};*Alb-Cre* AAV-HJV, n = 6). Data are presented as box plots with minimum to maximum whiskers and medians. Significances were presented relative to the indicated control with *$P < .05$, **$P < .01$, and ***$P < .001$.
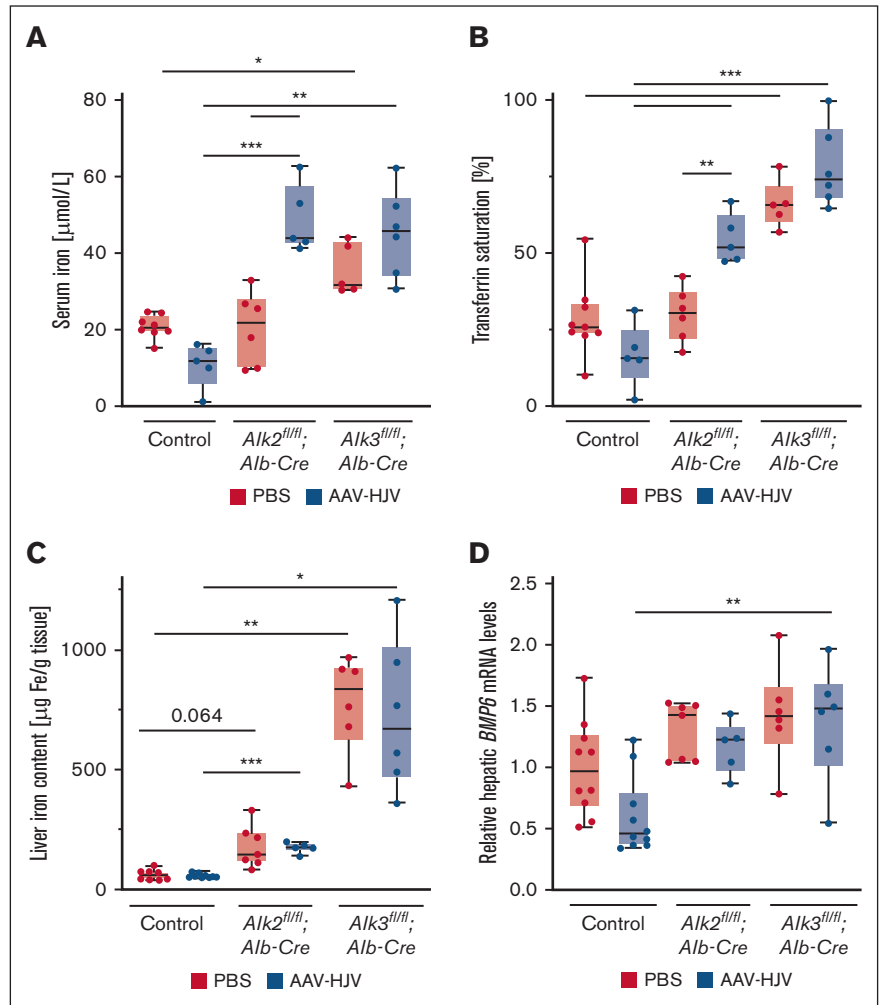
opposite effect: an increase in serum iron levels and transferrin saturation compared with PBS-injected littermates. This effect is in line with a trend of decreased hepcidin levels and the lack of increased BMP signaling transduction in these mice. The increase in serum iron, however, was stronger than the observed decrease in hepcidin. In *Alk3*^{fl/fl};*Alb-Cre* mice with already severe iron overload and increased iron parameters, AAV-HJV did not further change iron parameters compared with PBS-injected littermates.

As previously published,[8] liver iron content was increased in hepatocyte-specific *Alk3*-deficient mice and was modestly greater in *Alk2*^{fl/fl};*Alb-Cre* mice than in control animals, albeit not significant ($P = .06$) in contrast to our previous publication (characterization of 12-week-old female mice with a higher number of mice per group). The overexpression of HJV had no effect on liver iron content in all groups of mice (Figure 3C). The expression of the BMP ligand BMP6 is induced by the transcription factor NRF2 in response to iron loading in the liver.[24] Because prolonged HJV overexpression over 2 weeks had no effect on liver iron content, BMP6 mRNA levels were unchanged in AAV-HJV–injected controls, as expected. In AAV-HJV–injected *Alk3*^{fl/fl};*Alb-Cre* mice compared with AAV-HJV–injected controls, BMP6 levels were

higher (Figure 3D). This effect is provoked by the *Alk3* deficiency with severe iron overload, because *Bmp6* mRNA levels are induced in response to high hepatic iron loading.[8]

The amount of erythroid progenitor cells was determined by CD44/TER119 staining via flow cytometry analysis. A reduction in erythropoiesis as potential cause for the increased serum iron concentration was excluded, because erythropoiesis was similar in all groups of mice with and without AAV-HJV overexpression (data not shown). Therefore, the increase in serum iron in hepatocyte-specific *Alk2*-deficient mice is most likely caused by the hepcidin induction.

HJV overexpression increased SIC in control mice

Because serum iron content seemed to be more affected by HJV overexpression than liver iron content, we also investigated splenic iron content (SIC). In control mice, HJV overexpression led to an increase in SIC compared with PBS-injected controls, but not in *Alk2*^{fl/fl};*Alb-Cre* mice nor *Alk3*^{fl/fl};*Alb-Cre* mice injected with AAV-HJV (Figure 4A). Also, Prussian blue staining revealed iron retention in the spleen in HJV-overexpressing control mice (Figure 4B).
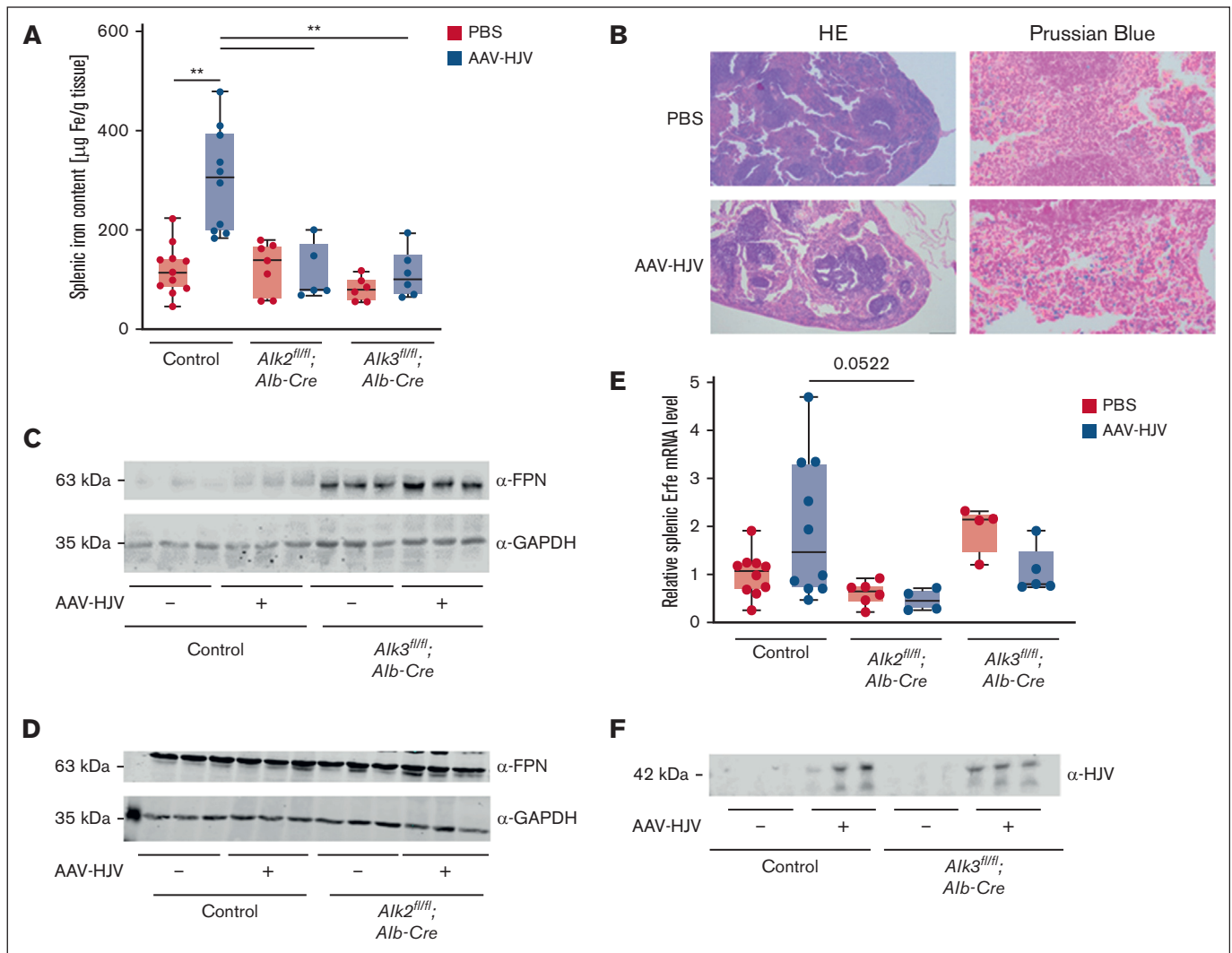
Figure 4. HJV overexpression causes splenic iron retention in control animals. (A) SIC was increased in control animals after HJV overexpression (control PBS, n = 11; control AAV-HJV, n = 10; $Alk2^{fl/fl}$;Alb-Cre PBS, n = 7; $Alk2^{fl/fl}$;Alb-Cre AAV-HJV, n = 5; $Alk3^{fl/fl}$;Alb-Cre PBS, n = 6; and $Alk3^{fl/fl}$;Alb-Cre AAV-HJV, n = 6). (B) Iron retention in the spleen was confirmed by Prussian blue staining. (C-D) Splenic ferroportin protein levels were determined by immunoblotting. GAPDH was used as internal control. (E) Splenic *Erfe* mRNA levels were determined by qRT-PCR. 18S ribosomal RNA was used as an internal control (control PBS, n = 10; control AAV-HJV, n = 10; $Alk2^{fl/fl}$;Alb-Cre PBS, n = 6; $Alk2^{fl/fl}$;Alb-Cre AAV-HJV, n = 4; $Alk3^{fl/fl}$;Alb-Cre PBS, n = 4; and $Alk3^{fl/fl}$;Alb-Cre AAV-HJV, n = 5). (F) Serum sHJV protein levels were determined by immunoblotting; n = 3 per group. Significances were presented relative to the indicated control with *$P < .05$, **$P < .01$, and ***$P < .001$.

Retention of iron in the spleen is known as an effect to prevent iron release in settings of hepcidin induction, here, mediated via AAV-HJV. In $Alk3^{fl/fl}$;Alb-Cre mice but not in $Alk2^{fl/fl}$;Alb-Cre mice, the protein expression of hepatic ferritin heavy chain, the iron storage protein, was further decreased after HJV overexpression (supplemental Figure 4A-D), which is in line with reduced hepatic hepcidin levels (Figure 2A). These data indicate that HJV overexpression causes hepcidin-mediated iron uptake and retention in the spleen of control mice but not in hepatocyte-specific $Alk2$- or $Alk3$-deficient mice. In order to determine whether splenic iron retention in AAV-HJV–injected control mice was caused by degradation of ferroportin, splenic ferroportin protein levels were analyzed. In $Alk3^{fl/fl}$;Alb-Cre mice, ferroportin protein expression was increased, which is in line with the reported severe iron overload of the phenotype and hepcidin deficiency, and the

injection of AAV-HJV had no impact on ferroportin protein levels (Figure 4C-D). In PBS-injected control mice, splenic ferroportin protein levels were low, and the overexpression of HJV slightly increased ferroportin protein levels. A potential explanation is the previously reported occlusion of ferroportin by hepcidin in AAV-HJV injected control mice.[25,26]

sHJV is increased by AAV-HJV overexpression

The effect of HJV-mediated hepcidin induction and splenic iron retention in control mice was absent in hepatocyte-specific $Alk2$- and $Alk3$-deficient mice. Interestingly, the overexpression of HJV suppressed *Hamp* mRNA levels in hepatocyte-specific $Alk3$-deficient mice and to a lesser extent in hepatocyte-specific $Alk2$-deficient mice but led to a serum iron and transferrin saturation increase in $Alk2^{fl/fl}$;Alb-Cre mice. Both findings indicate a reduced

activation of the BMP-SMAD signaling pathway. To validate whether ERFE, a known hepcidin antagonist, is responsible for the observed decrease in hepcidin expression in hepatocyte-specific *Alk3* mice, splenic *Erfe* mRNA levels were measured. In controls, the average of *Erfe* mRNA levels did not change upon HJV overexpression when compared to controls. In mice with hepatocyte-specific *Alk2* deficiency, splenic *Erfe* mRNA levels trended to be lower than in HJV-overexpressed controls (Figure 4E, $P = 0.0522$). sHJV is known to circulate in the plasma and act as a decoy receptor. It binds BMP ligands and thereby inhibits the induction of hepcidin and even leads to a decrease.[14] To consider this second possibility that plasmatic sHJV is responsible for the observed effects, sHJV was determined in serum samples of AAV-HJV–injected animals. In comparison with PBS-injected littermates, a 42-kDa sHJV form was detected in the sera of all AAV-HJV–injected mice (Figure 4F).

Discussion

HJV is a GPI-anchored protein of the repulsive guidance molecule family that acts as a BMP coreceptor. This work further investigated the role of HJV in iron homeostasis. We show that HJV signals via both BMP type I receptors ALK2 and ALK3 in vivo using an established model of AAV-mediated overexpression of HJV in hepatocyte-specific *Alk2-* or *Alk3*-deficient murine models. HJV overexpression in control mice causes an induction of HJV, sHJV, *Hamp*, and *Id1* mRNA levels, potentially by inducing pSMAD1/5/8 levels, along with decreased serum iron and transferrin saturation. Although the liver iron content remains unchanged, SIC increases. The requirement of ALK2 is shown, because there is no induction of BMP signaling in hepatocyte-specific *Alk2*-deficient mice after HJV overexpression. Interestingly, the contrary occurs: serum iron and transferrin saturation are highly induced, whereas *Hamp* mRNA levels show a decreased trend. These data indicate a further reduction in BMP-SMAD signaling. In mice with hepatocyte-specific *Alk2* deficiency, ALK3 is still present, but unable to mediate hepcidin induction via HJV. The necessity for ALK3 in HJV-mediated hepcidin induction is shown, because hepatocyte-specific *Alk3*-deficient mice have severely decreased BMP signaling that cannot be activated by HJV.

Our data are in line with results that have been published by Xia et al, who reported that HJV can use all three BMP type I receptors (ALK2, ALK3, and ALK6) in vitro to induce hepcidin expression.[13] To the best of our knowledge, in vivo studies have not yet been performed. Because only ALK2 and ALK3 are detected in the human liver[13] and are required for hepcidin induction and systemic iron homeostasis,[8] the role of these two receptors in HJV-mediated BMP signaling have been demonstrated in vivo. Previous studies suggest the formation of functionally active ALK3/ALK3 homodimers, ALK2/ALK3 heterodimers,[9] and ALK2/ALK2 homodimers.[7] In this manuscript it was demonstrated that both ALK2 and ALK3 are required for intact HJV signaling in vivo, suggesting that HJV may signal predominantly via the heterodimeric BMP type I receptor complex of ALK2/ALK3 and not via the homodimeric equivalent. Of note, in mice with hepatocyte-specific *Alk2* deficiency, signaling via ALK3/ALK3 homodimers still persists and hepcidin levels are maintained within normal, to mildly depleted, levels. Induction of the BMP pathway by iron or BMP ligands is, however, not feasible.[8] In contrast, in mice with a hepatocyte-specific *Alk3* deficiency, neither the ALK3/ALK3 homodimers nor

the ALK2/ALK3 heterodimers exist and BMP signaling is almost completely abrogated under basal, as well as stimulatory, conditions.[8,27] These data raise the question whether the iron overload phenotype of *Alk3*-deficient mice and *Hjv*-deficient mice is of similar severity. To date, no experiments have been performed to directly compare the iron overload phenotypes of *Alk3*^{fl/fl}*;Alb-Cre* mice with the iron overload phenotype of *Hjv* knockout mice. In terms of the importance of ALK2 and ALK3 in iron homeostasis, it is well known that ALK3 plays a more important role in vivo than ALK2.

It is therefore reasonable, and prior data indicate, that ALK3 homodimers play a more important role in hepcidin induction than ALK2 homodimers.[9] However, the hepatocyte-specific deletion of both *Alk2* and *Alk3* lead to a more severe iron overload phenotype than the hepatocyte-specific deletion of *Alk3* alone, suggesting that ALK2/ALK3 heterodimers are essential for HJV-mediated hepcidin signaling in vivo.[9]

Here, the overexpression of HJV in *Alk2*^{fl/fl}*;Alb-Cre* mice and in *Alk3*^{fl/fl}*;Alb-Cre* mice did not rescue the loss in BMP-SMAD signaling but led to an increase in circulating serum iron levels and transferrin saturation. The observed decrease in *Hamp* mRNA levels in hepatocyte-specific *Alk3*-deficient mice and to a lesser extent in hepatocyte-specific *Alk2*-deficient mice may be caused by unknown mechanisms induced by sHJV in vivo. Cleavage of HJV either at its furine cleavage site, the TMPRSS6 site, or at the autocleavage site, results in the smaller non–membrane bound form sHJV.[12,28] sHJV inhibits BMP signaling and reduces hepcidin expression *in vitro* by binding and sequestering BMP ligands, predominately BMP6. As a consequence, BMP6 cannot interact with its receptors, and fails to induce hepcidin expression.[29] sHJV can also bind BMP ligands in mice with hepatocyte-specific *Alk2* or *Alk3* deficiency. Therefore, binding of sHJV may result in reduced hepcidin expression and increased serum iron levels as we observed in mice with hepatocyte-specific *Alk2* or *Alk3* deficiency. In control animals, the overexpression of HJV also causes an increase in sHJV, but the BMP receptors required are functional and therefore BMP-SMAD signaling might be dominant over sHJV, and BMP ligand binding induces hepcidin expression.

One possible limitation of our study is that the overexpression of HJV may result in supraphysiological amounts of HJV and sHJV. All changes observed in iron homeostasis and BMP-SMAD signaling might not occur under physiological conditions. Increased HJV and sHJV levels may have an artificial effect on hepcidin synthesis and may cause a higher activation of BMP-SMAD signaling and hepcidin synthesis than in nonstimulated scenarios. However, to investigate the interaction of HJV in vivo, the method of AAV-HJV overexpression allows an in vivo setting, which is preferable to cellular models.

The observed effect of HJV overexpression on serum iron levels in hepatocyte-specific *Alk2*-deficient mice was impressive compared with the moderate hepcidin decrease. In comparison with hepatocyte-specific *Alk3*-deficient mice the induction was also more dominant. This may reflect the high baseline iron levels of hepatocyte-specific *Alk3*-deficient mice because of very low hepcidin levels and the severe iron overload phenotype of these mice.[8] Therefore, the overexpression of HJV and the increase in sHJV does not lead to a change in serum iron levels in hepatocyte-specific *Alk3*-deficient mice, because serum iron and transferrin

saturation are already saturated. The strong serum iron induction in mice with hepatocyte-specific *Alk2* deficiency injected with AAV-HJV raises the question of where the iron comes from. There are several hypotheses: first, HJV causes hepcidin-mediated inactivation of ferroportin and thereby decreases serum iron levels. In mice with *Alk2* deficiency, hepcidin induction does not occur because of deficiency of the BMP type I receptor ALK2. Therefore, ferroportin remains expressed and leads to an induction of serum iron. A second possibility might be that sHJV directly activates ferroportin in the setting of low hepcidin levels to increase iron absorption from the intestine, thereby increasing iron parameters in hepatocyte-specific *Alk2*-deficient mice. And third, another independent different mechanism could interfere and lead to a release of iron from iron storage cells. The hepcidin antagonist ERFE might be a potential candidate. The overexpression of HJV led to an induction of hepcidin. In splenic *Erfe* mRNA levels, there was a high variability observed in control mice in terms of induction and suppression of single values, which was missing in mice with hepatocyte-specific *Alk2* or *Alk3* deficiency.

In this study, the overexpression of HJV in control animals caused an induction in hepcidin expression and consequently splenic iron retention. These results are in contrast to those of Zhang et al, who reported that the AAV-mediated overexpression of HJV had no effect on iron status and hepcidin expression in wild-type mice.[30] In this study, mice on a C57BL/6 background were used, whereas Zhang et al characterized the effect of HJV overexpression in mice on a 129/SvEvTac background. Mice with a different genetic background show differences in iron homeostasis[31], and it is suggested that the contradictory results are a result of the different genetic mouse backgrounds used in both studies.

In conclusion, the data indicate that both ALK2 and ALK3 are functionally important for HJV-mediated hepcidin induction. sHJV induced by AAV-HJV can bind and thereby decrease BMP-SMAD signaling in vivo. HJV overexpression did not induce hepcidin expression in neither hepatocyte-specific *Alk2*- nor hepatocyte-specific *Alk3*-deficient mice, as it does in controls. Therefore, the use of the ALK2/3 heterodimer is most probably required for signaling and should be investigated in future studies.

Acknowledgments

Authorship

Contribution: D.Y.D. performed experiments, interpreted data, and wrote the manuscript; E.I.U., I.H., P.K., D.O., F.M.F., L.H.N., F.R., E.G., A.V.K., R.P., and I.F. performed experiments; U.K. and K.Z. interpreted data and wrote the manuscript; L.S. oversaw the study, performed experiments, interpreted data, and wrote the manuscript; and A.U.S. planned the project, conceived and oversaw the study, performed experiments, interpreted data, and wrote the manuscript.

Conflict-of-interest disclosure: K.Z. declares that the Department of Anaesthesiology, Intensive Care Medicine & Pain Therapy of the University Hospital Frankfurt, Goethe University received support from B. Braun Melsungen, CSL Behring, Fresenius Kabi, and Vifor Pharma for the implementation of Frankfurt's Patient Blood Management program. K.Z. has received honoraria for participation in advisory board meetings for Haemonetics and Vifor; received speaker fees from CSL Behring, Masimo, Pharmacosmos, Boston Scientific, Salus, iSEP, and Edwards and GE Healthcare; and serves as the principal investigator of the EU-Horizon 2020 project ENVISION (Intelligent plug-and-play digital tool for real-time surveillance of patients with COVID-19 and smart decision-making in intensive care units) and the Horizon Europe 2021 project COVend (Biomarker and AI-supported FX06 therapy to prevent progression from mild and moderate to severe stages of COVID-19). The remaining authors declare no competing financial interests.

ORCID profiles: D.Y.D., 0009-0009-8783-6823; E.I.U., 0000-0002-1028-7442; P.K., 0009-0000-7561-4312; U.K., 0000-0001-9845-3099; A.v.K., 0000-0002-5831-0365; I.F., 0000-0003-1881-3635.

Correspondence: Andrea U. Steinbicker, Department of Anesthesiology, Intensive Care and Pain Medicine, University Hospital Frankfurt, Goethe University Frankfurt, Theodor-Stern-Kai 7, Building 13, 60590 Frankfurt Am Main, Germany; email: steinbicker@em.uni-frankfurt.de.

References

1. Pigeon C, Ilyin G, Courselaud B, et al. A new mouse liver-specific gene, encoding a protein homologous to human antimicrobial peptide hepcidin, is overexpressed during iron overload. *J Biol Chem*. 2001;276(11):7811-7819.

2. Srole DN, Ganz T. Erythroferrone structure, function, and physiology: iron homeostasis and beyond. *J Cell Physiol*. 2021;236(7):4888-4901.

3. Wang CY, Xu Y, Traeger L, et al. Erythroferrone lowers hepcidin by sequestering BMP2/6 heterodimer from binding to the BMP type I receptor ALK3. *Blood*. 2020;135(6):453-456.

4. Nemeth E, Tuttle MS, Powelson J, et al. Hepcidin regulates cellular iron efflux by binding to ferroportin and inducing its internalization. *Science*. 2004;306(5704):2090-2093.

5. Nemeth E, Ganz T. Hepcidin-ferroportin interaction controls systemic iron homeostasis. *Int J Mol Sci*. 2021;22(12):6493.

6. Canali S, Zumbrennen-Bullough KB, Core AB, et al. Endothelial cells produce bone morphogenetic protein 6 required for iron homeostasis in mice. *Blood*. 2017;129(4):405-414.

7. Pettinato M, Dulja A, Colucci S, et al. FKBP12 inhibits hepcidin expression by modulating BMP receptors interaction and ligand responsiveness in hepatocytes. *Am J Hematol*. 2023;98(8):1223-1235.

8. Steinbicker AU, Bartnikas TB, Lohmeyer LK, et al. Perturbation of hepcidin expression by BMP type I receptor deletion induces iron overload in mice. *Blood*. 2011;118(15):4224-4230.

9. Traeger L, Gallitz I, Sekhri R, et al. ALK3 undergoes ligand-independent homodimerization and BMP-induced heterodimerization with ALK2. *Free Radic Biol Med*. 2018;129:127-137.

10. Xiao X, Dev S, Canali S, et al. Endothelial bone morphogenetic protein 2 (Bmp2) knockout exacerbates hemochromatosis in homeostatic iron regulator (Hfe) knockout mice but not Bmp6 knockout mice. *Hepatology*. 2020;72(2):642-655.

11. Babitt JL, Huang FW, Wrighting DM, et al. Bone morphogenetic protein signaling by hemojuvelin regulates hepcidin expression. *Nat Genet*. 2006;38(5):531-539.

12. Niederkofler V, Salie R, Arber S. Hemojuvelin is essential for dietary iron sensing, and its mutation leads to severe iron overload. *J Clin Invest*. 2005;115(8):2180-2186.

13. Xia Y, Babitt JL, Sidis Y, Chung RT, Lin HY. Hemojuvelin regulates hepcidin expression via a selective subset of BMP ligands and receptors independently of neogenin. *Blood*. 2008;111(10):5195-5204.

14. Babitt JL, Huang FW, Xia Y, Sidis Y, Andrews NC, Lin HY. Modulation of bone morphogenetic protein signaling in vivo regulates systemic iron balance. *J Clin Invest*. 2007;117(7):1933-1939.

15. Healey EG, Bishop B, Elegheert J, Bell CH, Padilla-Parra S, Siebold C. Repulsive guidance molecule is a structural bridge between neogenin and bone morphogenetic protein. *Nat Struct Mol Biol*. 2015;22(6):458-465.

16. Mishina Y, Hanks MC, Miura S, Tallquist MD, Behringer RR. Generation of Bmpr/Alk3 conditional knockout mice. *Genesis*. 2002;32(2):69-72.

17. Dudas M, Sridurongrit S, Nagy A, Okazaki K, Kaartinen V. Craniofacial defects in mice lacking BMP type I receptor Alk2 in neural crest cells. *Mech Dev*. 2004;121(2):173-182.

18. Traeger L, Enns CA, Krijt J, Steinbicker AU. The hemochromatosis protein HFE signals predominantly via the BMP type I receptor ALK3 in vivo. *Commun Biol*. 2018;1:65.

19. Gao J, Chen J, De Domenico I, et al. Hepatocyte-targeted HFE and TFR2 control hepcidin expression in mice. *Blood*. 2010;115(16):3374-3381.

20. Torrance J, Bothwell T, Cook J. *Methods in Hematology*. Churchill Livingstone; 1980:104-109.

21. Pfaffl MW. A new mathematical model for relative quantification in real-time RT-PCR. *Nucleic Acids Res*. 2001;29(9):e45.

22. Krijt J, Frýdlová J, Gurieva I, et al. Matriptase-2 and hemojuvelin in hepcidin regulation: in vivo immunoblot studies in mask mice. *Int J Mol Sci*. 2021;22(5):2650.

23. Snyder RO, Miao CH, Patijn GA, et al. Persistent and therapeutic concentrations of human factor IX in mice after hepatic gene transfer of recombinant AAV vectors. *Nat Genet*. 1997;16(3):270-276.

24. Lim PJ, Duarte TL, Arezes J, et al. Nrf2 controls iron homeostasis in haemochromatosis and thalassaemia via Bmp6 and hepcidin. *Nat Metab*. 2019;1(5):519-531.

25. Aschemeyer S, Qiao B, Stefanova D, et al. Structure-function analysis of ferroportin defines the binding site and an alternative mechanism of action of hepcidin. *Blood*. 2018;131(8):899-910.

26. Pantopoulos K. Hepcidin inhibitis iron efflux from duodenal ferroportin and indirectly promotes iron-dependent DMT1 degradation. In: *BioIron Society Meeting, Poster 60*. Kostas Pantopoulos; 2023.

27. Mayeur C, Lohmeyer LK, Leyton P, et al. The type I BMP receptor Alk3 is required for the induction of hepatic hepcidin gene expression by interleukin-6. *Blood*. 2014;123(14):2261-2268.

28. Silvestri L, Pagani A, Camaschella C. Furin-mediated release of soluble hemojuvelin: a new link between hypoxia and iron homeostasis. *Blood*. 2008;111(2):924-931.

29. Nili M, Shinde U, Rotwein P. Soluble repulsive guidance molecule c/hemojuvelin is a broad spectrum bone morphogenetic protein (BMP) antagonist and inhibits both BMP2- and BMP6-mediated signaling and gene expression. *J Biol Chem*. 2010;285(32):24783-24792.

30. Zhang AS, Gao J, Koeberl DD, Enns CA. The role of hepatocyte hemojuvelin in the regulation of bone morphogenic protein-6 and hepcidin expression in vivo. *J Biol Chem*. 2010;285(22):16416-16423.

31. Saha P, Xiao X, Li Y, et al. Distinct iron homeostasis in C57BL/6 and Balb/c mouse strains. *Phys Rep*. 2020;8(9):e14441.